A NEW DAMAGE-CONTROL TARGET DISPLACEMENT PROCEDURE FOR DIRECT DISPLACEMENT-BASED DESIGN OF CIRCULAR REINFORCED CONCRETE BRIDGE PIER

MOHD RITZMAN ABDUL KARIM & ZHAOHUI HUANG
Department of Civil and Environmental Engineering, Brunel University, UK.

ABSTRACT
In this paper, a new perspective procedure to determine the damage-control target displacement for circular reinforced concrete (RC) bridge pier is proposed by considering the new approach of damage-control limit states (DCLS). The new approach of DCLS is explored by integrating existing damage-control concrete strain limit with recently proposed damage-control reinforcement strain limit. Modification of yield displacement and modified plastic-hinge along with new DCLS is used to estimate the damage-control target displacement for a circular RC bridge pier. Three-dimensional (3D) finite element (FE) model has been developed to validate the damage-control target displacement subject to ground motion based on a nonlinear time-history (NLTH) analysis. The 3D FE model is updated to achieve a reasonable relationship between numerical, analytical, and outcomes found in the literature. It is worth noting that the proposed procedure manages to estimate an improved damage-control target displacement for 7.0 m, 11.0 m and 13.0 m height of circular RC bridge pier. The influence of new reinforcement limit strain along with both modification of yield displacement and plastic-hinge contributes to providing better results. The result shows that new DCLS were efficient to predict damage-control target displacement, consistent with FE analysis result.
Keywords: circular RC bridge pier, damage-control limit states, damage-control target displacement, plastic-hinge region, yield displacement.

1 INTRODUCTION

In the current context of seismic design, displacement-based design method has been developed over the past decades in order to overcome the limitations of the present design method (i.e. force-based design) [1]–[4]. The displacement-based design method relies on the design limit states and performance level [5]. The fundamental theory of the displacement-based method is to design structures to achieve specific performance level and design limit state under different earthquake conditions. The structural performance levels can be divided into four different categories [5]: (a) fully operational; (b) operational; (c) life safe and (d) near collapse. However, it needs some modification to include 'damage control' performance level, for economic reasons [5–7].

'Damage control' can be highlighted as structures that face damage is repairable after seismic events. To further understand the 'damage control' performance level, the relationship between performances levels and structures limit states is needed. To ensure the structural performance levels can be controlled during an earthquake event, it is vital to consider the damage-control limit state (DCLS) at the design limit state. Although the DCLS is not directly addressed in design codes, consideration of this limit state is highly recommended. The consideration of DCLS is to ensure the damage towards the structures is satisfactory; the repairable cost is acceptable and should be less than replacing the new reinforced concrete (RC) bridge pier. The structures damage may include concrete spalling at the concrete cover.

Direct displacement-based design (DDBD) uses the DCLS as part of the design process in order to determine the target displacement for damage control. To be used in the design stage

ISSN: 2041-9031 (paper format), ISSN: 2041-904X (online), http://www.witpress.com/journals
DOI: 10.2495/SAFE-V9-N3-249-260

for DDBD method, DCLS is governed by both material strain, which is the ultimate concrete compression strain, and ultimate reinforcement tensile strain. The energy balance approach developed by Mander *et al*. [8] is used to estimate the ultimate concrete reinforcement strain. However, prediction of the ultimate reinforcement limit strain has been limited [9–10].

In order to overcome insufficient data in the literature, studies on the reinforcement strain limit for single-degree-of-freedom (SDOF) RC bridge pier have been carried out in recent years. The research conducted by Goodnight *et al*. [10] provides a better model to understand the importance of reinforcement limit strain focused on bar buckling. DCLS is used to determine the damage-control target displacement, $\Delta_{T,DC}$ for DDBD method. Therefore, this paper attempts to explore and predict the $\Delta_{T,DC}$, based on the integration of new reinforcement limit strain proposed by Goodnight *et al*. [10] and existing concrete compression strain [8], modified plastic-hinge region [11] and modification of yield displacement [12] for a bridge pier.

2 REVIEW OF DCLS

Formerly, 'life safe' performance level has been adopted in order to design structures. However, after the 1995 Kobe earthquake, many structures experienced extensive and beyond-repair damage. Therefore, to overcome this issue, DCLS is required to be adopted as part of the design. Consideration of DCLS is to ensure that the structure remains functional and restrains the structures that suffered from excessive damage after earthquake events.

Traditionally, the serviceability limit state [5–6, 13] is considered in the design stage. Despite that, higher restriction limit is weighed in favour of to determine the target displacement for DDBD method. Figure 1 shows an example of the force–displacement relationship for the ductile element (RC bridge pier) highlighted the damage-control target displacement, $\Delta_{T,DC}$ position and yield displacement, Δ_y. In DDBD method, the DCLS is based on the material strain limit; damage-control concrete compression strain limit, $\varepsilon_{c,dc}$ and damage-control reinforcement tensile strain limit, $\varepsilon_{s,dc}$. The damage-control concrete compression limit strain can be defined as the compression strain that represents significant damage (spalling of concrete cover, minor cracks, etc.) to the concrete, but at this damage level it is still repairable.

The experimental research shows that the above assumption is subjective and depends on the transverse reinforcement details provided in the RC bridge pier. According to current limit states definitions, some authors considered the value of 0.018 as an approximation of damage-control concrete compression strain [9]. The damage-control reinforcement tensile

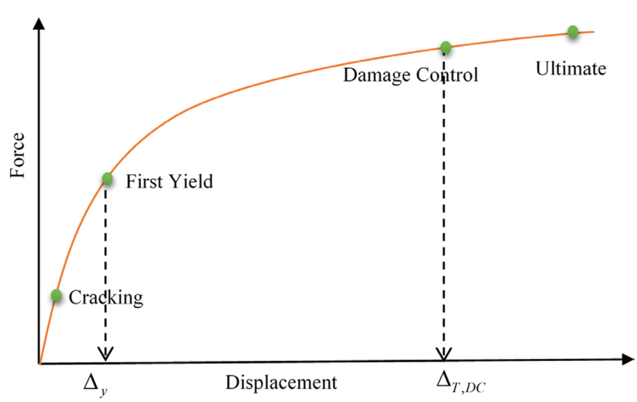

Figure 1: Force–displacement relationships.

strain can be highlighted as strain at the peak tension strain during loading cycle in which buckling of the reinforcement starts to develop. The quantification of the reinforcement tensile strain is still difficult, due to insufficient experimental data, particularly at damage-control level [10]. Therefore, based on previous research conducted in 1996 [14], the value of 0.060 for the DCLS related to the tensile reinforcement strain was assumed [9].

3 CURRENT PROCEDURE TO DETERMINE DAMAGE-CONTROL TARGET DISPLACEMENT

In DDBD approach, one of the most important procedure is to determine the target displacement for a single RC bridge shown in Fig. 2a and b. Based on the plastic-hinge method [5], strain-based target displacement [6] can be determined along the transverse axis of the bridge pier.

The strain-based target displacement, Δ_T is given by eqn (1) [5–6]. In eqn (1), Δ_y is the yield displacement of the bridge pier, ϕ_t and ϕ_y is the target and yield curvature, respectively, L is the pier height and L_p is the plastic hinge length.

$$\Delta_T = \Delta_y + \left(\phi_t - \phi_y\right) L_p \; L. \tag{1}$$

Recent studies show that eqn (1) can be used to determine the target displacement for DCLS [6, 15]. In DDBD approach highlighted in [15], based on the bridge pier geometry and reinforcement detailing, the limit state is defined from the moment–curvature analysis. Figure 2c shows the limit states definition from moment curvature.

In this figure, the yield curvature, ϕ_y, is determined by extrapolating the first yield curvature, $\phi_y^{'}$ at the nominal flexural moment, M_n and ϕ_s indicate serviceability target curvature. Damage-control target curvature, ϕ_{dc} is determined when the damage-control concrete compression strain, $\varepsilon_{c,dc}$ reaches 0.018 or damage-control reinforcement tensile strain, $\varepsilon_{s,dc}$ reaches 0.060. This position indicates the ultimate moment, M_u. Once the curvature is attained, the strain-based target displacement can be used to determine $\Delta_{T,DC}$ by replacing the target curvature ϕ_t to ϕ_{dc} damage-control target curvature. Thus, the $\Delta_{T,DC}$ can be estimated using eqn (2) [5–6].

$$\Delta_{T,DC} = \Delta_y + \left(\phi_{dc} - \phi_y\right) L_p \; L. \tag{2}$$

In eqns (1) and (2), L_p defined as a plastic hinge [5, 9] is given by eqns (3) and (4). The highest value of plastic-hinge length based on both eqns (3) and (4) is used to determine the $\Delta_{T,DC}$. To ensure the compatibility, eqns (3) and (4) should be only for stress input in MPa units.

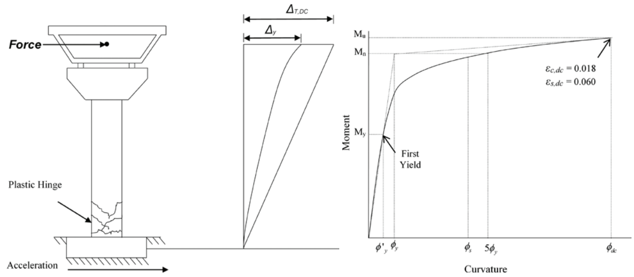

(a) (b) (c)

Figure 2: Studied RC bridge pier (a), related displacements (b) and limit states definition from moment curvature (c).

$$L_p = 0.08L + 0.022 f_y d_{bl}. \tag{3}$$

$$L_p = 0.044 f_y d_{bl}. \tag{4}$$

First, DCLS is determined. Then, the ϕ_{dc} is computed as follows [5–6]:

$$\phi_{dc} = \min\left[\left(\varepsilon_{c,dc}/c\right), \left(\varepsilon_{s,dc}/D-c\right)\right], \tag{5}$$

where c is the neutral axis depth, D the diameter of the bridge pier. Utilising the ϕ_{dc} formulated in Eqn (5), Kowalsky [9] suggested that the ϕ_{dc} can be defined based on the following eqn (6):

$$\phi_{dc} = \frac{1}{D}\left(0.068 - 0.068\left(P/f'_c A_g\right)\right). \tag{6}$$

where $P/f'_c A_g$ is the RC bridge pier axial load ratio (ALR) based on the material used given by eqn (7) [5]. However, eqn (6) can be used if the axial load and longitudinal reinforcement ratios (LLRs) are within the limits of the proposed equation (eqn (6)), i.e. 0.1–0.4 for ALR, and 1–4% LRR. The neutral axis depth can be obtained by the following expression:

$$c = 0.2D\left(1 + 3.25\left(P/f'_c A_g\right)\right). \tag{7}$$

In order to determine the DCTD, highlighted in eqn (2), yield curvature and yield displacement are required. Yield curvature, ϕ_y is given by the following equation:

$$\phi_y = 2.25\,\varepsilon_y/D. \tag{8}$$

where ε_y is the yield strain of the longitudinal reinforcement [4–5, 16].

The yield displacement Δ_y is given by eqn (9) where L_{sp} is the strain penetration, which is given by eqn (10) [4, 6, 14], and L is the pier height.

$$\Delta_y = \left(\phi_y (L + L_{sp})^2\right)/3. \tag{9}$$

$$L_{sp} = 0.022\, f_y\, d_{bl}. \tag{10}$$

In eqn (10), L_{sp} is a function of the diameter of the longitudinal reinforcement d_{bl} and yield stress of the longitudinal reinforcement f_y. Using the results from eqns (5), (7)–(9), eqn (2) is used to estimate the $\Delta_{T,DC}$.

4 PROPOSED PROCEDURE OF DAMAGE-CONTROL TARGET DISPLACEMENT

The design displacement for a SDOF RC bridge pier depends on the performance limit state, such as the basis of material strains, ductility or the drift. Due to the lack of previous experimental data, the study conducted by Goodnight *et al*. [10] developed a new expression to predict reinforcement tensile limit strain based on the peak of tensile towards bar buckling. The expression is given by eqn (11) [10].

$$\varepsilon_{s,dc} = 0.03 + 700\rho_s\left(f_{yhe}/E_s\right) - 0.1\left(P/f'_{ce} A_g\right), \tag{11}$$

where ρ_s is the transverse reinforcement ratio, f_{yhe}/E_s the expected yield stress of the transverse reinforcement and $P/f'_{ce}A_g$ is the bridge pier ALR based on the material used. Eqn (11) has been developed based on peak tension strain prior to bar buckling during cyclic analysis, in order to determine the displacement capacity for RC bridge pier. This reinforcement tensile strain has been adopted in this proposed study due to one of the causes of damages towards reinforcement, and in the RC bridge pier is related to the bar buckling. Eqn (11) is used to determine the ϕ_{dc}.

Mander *et al.* [8] suggested that the specific concrete compression for confined concrete can be estimated using the dissipation energy balance approach. Thus, the concrete compression strain for damage control to be used to determine ϕ_{dc} is defined by eqn (12).

$$\varepsilon_{c,dc} = 0.004 + 1.4\left(\rho_v\, f_{yh}\, \varepsilon_{su} / f'_{cc}\right). \tag{12}$$

Eqn (12) represents the concrete compressive strain for damage-control, and is a function of volumetric transverse ratio, ρ_v, the ultimate strain of steel reinforcement in the transverse direction, ε_{su}, the yield stress of transverse steel reinforcement, f_{yh}, the compressive strength of unconfined concrete, f'_c, the compressive strength of confined concrete, f'_{cc} and confinement stress, f_1. The compressive strength of confined concrete is given by eqn (13) and the confinement stress is given by eqn (14).

$$f'_{cc} = f'_c\left(2.254\sqrt{1+\left(7.94 f_1/f'_c\right)} - 2\left(f_1/f'_c\right) - 1.254\right). \tag{13}$$

$$f_1 = 0.5\,\rho_v\, f_{yh}\,. \tag{14}$$

Priestley and Kowalsky [17] believe that the concrete compression strain limit provided by energy balance developed by Mander *et al.* [8] is conservative. The focus of this research is to investigate the damage-control target displacement based on the newly proposed procedure. Several modifications have been considered in the proposed procedure in order to determine the significant damage-control target displacement result. Combination of new yield displacement [12], and the modified plastic-hinge length [11] is considered to determine the $\Delta_{T,DC}$ for RC bridge pier. Equation (15) is used to determine the $\Delta_{T,DC}$.

$$\Delta_{T,DC} = \Delta_y + \left(\phi_{dc} - \phi_{y,eff}\right) Lpr\; L_{eff}\,. \tag{15}$$

In eqn (15), ϕ_{dc} is given by eqn (5) and Lpr is the triangular plastic hinge length given by eqns (20) and (21). L_{eff} is the effective pier height, given by eqn (18), where L is the pier height and L_{sp} the strain penetration length given by eqn (19). The effective yield curvature, $\phi_{y,eff}$ and Δ_y are based on new approximation. The effective yield curvature $\phi_{y,eff}$ expression shown is given by:

$$\phi_{y,eff} = \phi_y \times MF(f'_c) \times MF(n) \times MF(p). \tag{16}$$

In eqn (16), MF is the modification factor given in Sheikh *et al.* [18]. The yield displacement used in this research is given by [12]

$$\Delta_y = \left(2.0 \times \left(\varepsilon_y / D^{1.1}\right) \times MF(f'_c) \times MF(n) \times MF(p) \times L_{eff}^{\;2}\right)/3, \tag{17}$$

where L_{eff} is the effective height of a bridge pier given by eqn (18).

$$L_{eff} = L + L_{sp}. \tag{18}$$

A compatible strain penetration length L_{sp} is required in order to ensure a fully compatible model used in this research. Modified strain penetration length is given by [11]:

$$L_{sp} = 0.152 \times (1 - P/f_c^{'} A_g - L/16D) \times \left(f_{ye} d_{bl} \Big/ \sqrt{f_{ce}^{'}}\right), \tag{19}$$

where f_{ye} is the expected yield strength of longitudinal reinforcement, A_g the gross area of concrete, P a compressive axial load, $f_c^{'}$ the concrete strength, $f_{ce}^{'}$ the foundation concrete strength and d_{bl} the diameter of the longitudinal reinforcement. The plastic-hinge length is needed to compute the $\Delta_{T,DC}$. Based on the same study by Goodnight *et al.* [11], separate triangular plastic-hinge length Lpr is developed based on tension and compression of the material. Equation (20) highlights the tensile plastic hinge length, Lpr_t and eqn (21) highlights the compressive plastic hinge length Lpr_c.

$$Lpr_t = 2kL_c + 0.75D. \tag{20}$$

$$Lpr_c = 2kL_c, \tag{21}$$

where

$$k = 0.2\left(f_u/f_y - 1\right) \le 0.08. \tag{22}$$

$$L_c = L. \tag{23}$$

In eqn (22), f_u is the ultimate stress of longitudinal reinforcement and f_y is the yield stress of longitudinal reinforcement. The final choice between eqns (20) and (21) to represent triangular plastic-hinge length Lpr is based on which of them governs the minimum value of strain to represent ϕ_{dc}, as highlighted in eqn (5). The calculation steps proposed in this model for determining damage-control target displacement can be summarised as follows:

1. Calculate effective yield curvature, $\phi_{y,eff}$ (eqn (16)), effective length, L_{eff}, (eqn (18)) and modified strain penetration length, L_{sp} (eqn (19)).
2. Calculate yield displacement, Δ_y (eqn (17)).
3. Determine the damage-control limit strain based on eqns (11) and (12).
4. Calculate damage-control target curvature, ϕ_{dc} (eqn (5)).
5. Calculate triangular plastic-hinge length, Lpr (eqns (20) and (21)) and determine which strain governs the design and calculate $\Delta_{T,DC}$ (eqn (15)).

5 FINITE ELEMENT MODEL

5.1 Development of a 3D model

Three-dimensional (3D) finite-element (FE) models were developed using FE software, ABAQUS [19]. The RC bridge pier and the foundation were modelled using 8-node solid concrete elements with reduced integration (C3D8R) shown in Fig. 3a. Mesh sensitivity analysis was conducted in order to determine the proper size of elements. A proper selection of

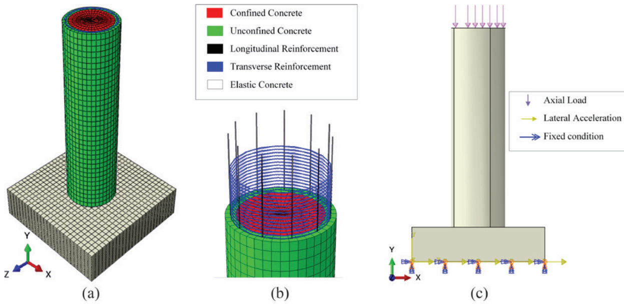

Figure 3: FE model developed in this research: overall view (a) details of the upper part (b) and lateral view with boundary conditions and loads (c).

mesh is adapted to ensure mesh size between the foundation, the pier and the loading that can improve the accuracy of the 3D model. Reinforcement bar of the bridge pier was modelled as 2-node steel truss elements (T3D2). The transverse reinforcement was modelled using individual spiral along the height of the RC bridge pier and through the foundation based on strain penetration length. The coloured regions indicate that different material model was assigned to the FE model shown in Fig. 3b. The reinforcement bars are embedded into RC bridge pier using embedded option, available in ABAQUS [19], to ensure the perfect interaction between reinforcement and concrete [20–21]. Constraint condition was modelled as a fixed boundary condition at the bottom of the foundation in order to replicate the experimental setup in the previous study. Axial load was applied on top of the RC bridge pier in the vertical direction. Lateral acceleration was modelled as amplitude in order to match the condition of acceleration time history in real seismic condition. Lateral acceleration was applied to the model, by imposing acceleration time-history at the bottom surface of the foundation as shown in Fig. 3c.

The elastic modulus for concrete and reinforcing based on uniaxial stress–strain bars was defined based on the Eurocode 2 (EC2) [22]. Young's modulus of the concrete E_c was assumed to be 35,000 MPa, according to EC2. The stress–strain relationship for the steel reinforcement bar is based on the bilinear relationship in EC2 [22]. The Young's modulus and Poisson's ratio used for reinforcement are 210 kN/mm^2 and 0.3, respectively. Concrete damage plasticity (CDP) was adopted in this study in order to simulate the inelastic behaviour of RC bridge piers and to utilise the nonlinear response of concrete behaviour.

CDP is capable of capturing the damage associated with the failure mechanism occurs in concrete with a moderate amount of confining pressure. CDP model used a yield function developed by Lubliner *et al*. [23] and modified by Lee and Fenves [24] to consider several concepts of strength under tension and compression [25]. The RC bridge pier was divided into three different regions to represent the confined concrete, unconfined concrete and the reinforcement. The compressive strength for confined and unconfined concrete used in this research is based on a model developed by Mander *et al*. [8]. The compressive and tension damage parameters for concrete were calculated based on the method suggested by Jankowiak and Lodygowski [26]. The stress–strain is based on the scalar damage elasticity where, the scalar stiffness degradation range from zero (undamaged) to one (fully damaged), thus, reduction in elastic stiffness.

5.2 Validation of the FE model

Validation FE model needs to be conducted in order to ensure the accuracy of the FE model. Analysis has been conducted and validated with experimental data found in the literature. The experimental cyclic force–displacement result from Lehman *et al*. [27] is compared with the

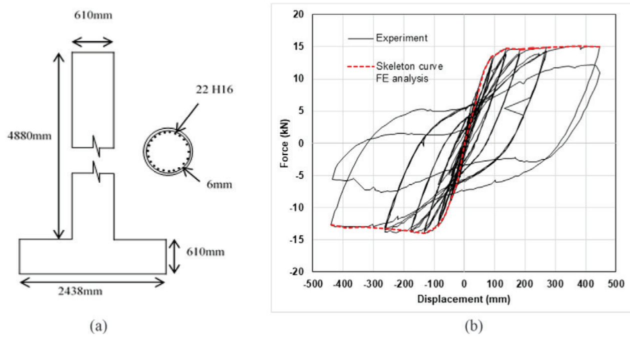

Figure 4: Details of the specimen from Lehman *et al*.'s test (a) and comparison with numerical results (b).

predicted backbone response from FE analysis. FE models are developed based on data available from experimental developed by Lehman *et al*. [27]. Figure 4a shows the specimen details for FE model validation. Based on Lehman *et al*.'s test, the column was 610 mm in diameter, and the reinforcement consisted of 22 bars with 16 mm diameter (22 H16) and 32 spiral reinforcements with equal spacing and 6 mm diameter. The concrete strength and axial load applied to the column were 30 MPa and 877 kN, respectively. Then, a controlled increasingly horizontal displacement was applied at the free end of the column. Figure 4b shows the FE analysis result compared with the experimental study. The figure shows the FE skeleton curve manages to predict the same peak envelope predicted by the experimental test result. It is evident that an excellent agreement between the FE model and experimental works was achieved.

6 RESULTS

6.1 Application to earthquake ground motions

Three FE analyses are based on the seismic response from the ABAQUS [19] software, incorporating several parameters to predict target displacement by applying seven ground motions. In order to validate the proposed model, the NLTH analysis was used to obtain the real seismic response of the FE model subjected to numbers of ground motions. The seven ground motion records were selected randomly from the Pacific Earthquake Engineering Research Center database. Figure 5a illustrates the acceleration response spectra with 5% damping for the selected ground motions. In Fig. 5b, two time-history accelerations (EL-Centro and Loma Prieta earthquakes) are depicted. The main parameters considered in this section are concrete strength, LRR, transverse reinforcement ratio and ALR. For FE analysis, the $\Delta_{T,DC}$ for Kowalsky's is extracted based on the strain predicted by the proposed model. Kong [15] conducted an analysis in North Carolina State University in 2017, while Kowalsky [9] conducted an analysis in 2000. Based on both previous researches, three specimens (with 1%, 2% and 3% of LRR) were used as a reference for validation.

In the analysis, Kong [15] evaluated the target displacement using bridge metadata for rapid direct-displacement based assessment procedure and validated it using NLTH. The details of the specimens are as follows: the concrete compressive strength is 30 MPa, the yield strength of reinforcement steel bars is 420 MPa, the longitudinal bar diameter is 35 mm and the transverse volumetric reinforcement ratio is 1%. An ALR of 8% was adopted with three different longitudinal steel ratios (1%, 2% and 3%) as input data for the RC bridge pier modelling using

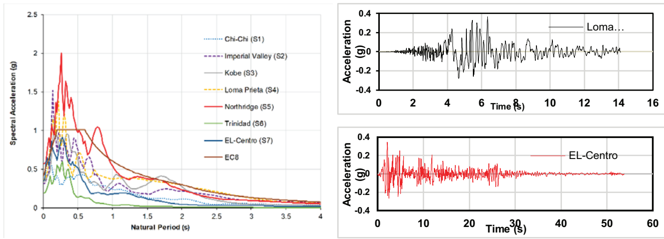

(a) (b)

Figure 5: Acceleration response spectra with 5% damping of considered earthquakes compared to the Eurocode 8 spectrum (EC8) [28] (a); time history recordings of Loma Prieta and El-Centro earthquakes (b).

ABAQUS [19]. Similar material details were used for Kowalsky's model. However, $\Delta_{T,DC}$ was determined based on the ϕ_{dc} against ALR graph developed in that study or using eqn (6) [9].

In Fig. 6, the $\Delta_{T,DC}$ is shown for three LRR values (1%, 2% and 3%) and for three different heights of RC bridge pier (7 m, 11 m, and 13 m).

The proposed model was compared with the FE-NLTH results obtained with the seven ground motions selected in this study and with the analytical models used in Kowalsky [9] and Kong [15]. A comparison with FE-NLTH analyses for the seven ground motions was also carried out. Figure 6 shows that the $\Delta_{T,DC}$ from the Northridge response (S5) resulted significantly higher compared with the proposed model and the other ground motions. This may be due to the peak ground acceleration of the Northridge record, which is higher than the others. While the response with Trinidad record (S6) resulted slightly lower than the others. For the remaining five seismic recordings, the proposed model provided convincing outcomes for an accurate estimate of $\Delta_{T,DC}$, much more convincing than the Kowalsky and the Kong models, which provide remarkably higher values.

The proposed model gave relatively accurate results, with a minimum error of −1.32%, which was partly due to the main parameters considered values. These phenomena indicate that the combination of new reinforcement tensile strain and existing concrete compression strain enhance the prediction of $\Delta_{T,DC}$.

6.2 The error of the proposed procedure

The proposed procedure described earlier for determining the DCTD has been applied to the single RC bridge piers. This section is mainly dedicated to discover the error percentage between the proposed procedure and FE-NLTH analysis. By doing so, it can indicate how effective the proposed procedure, compares with real seismic analysis.

Table 1 shows the error percentage of the DCTD for the proposed model, Δ_{pro} and the FE model, Δ_{FE} for all ground motion. In Table 1, the FE model undergoes seven sets of ground motions highlighted in Fig. 5. The parameters for the material used is based on the parameter highlight in Section 6.1. The overall ratio of error percentage is <10% for three different heights of RC bridge pier. Therefore, it verifies the accuracy of the FE model and the accuracy of the proposed procedure to estimate the DCTD for RC bridge pier. Table 2 shows the error percentage of the DCTD for the proposed model and the previous model considered in this study. The error percentage is high for both the previous models. This phenomenon may be due to the proposed procedure is taken into consideration of the new DCLSs along with effective yield

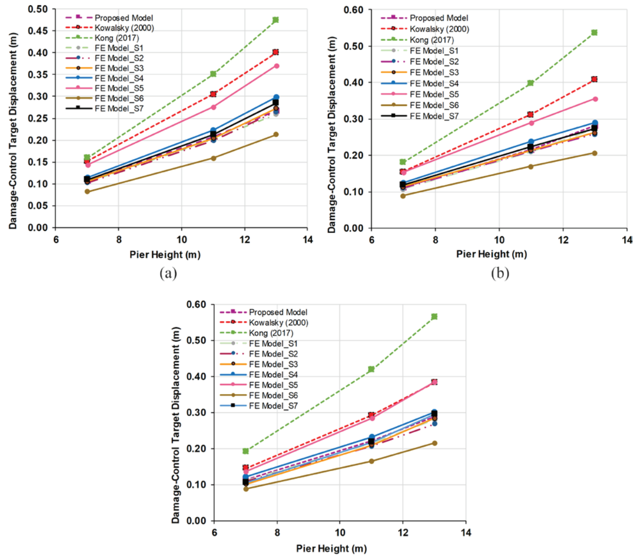

(a) (b) (c)

Figure 6: Comparison of the predicted $\Delta_{T,DC}$ by the proposed model, NLTH-FE analyses (FE Models) and previous models by Kowalsky and by Kong under 1% LRR (a), 2% LRR (b) and 3% LRR (c).

Table 1: Error percentage for proposed model Δ_{pro}, and FE model, Δ_{FE}.

		Error percentage, $\Delta_{pro}/\Delta_{FE}(\%)$						
Ground motions		**S1**	**S2**	**S3**	**S4**	**S5**	**S6**	**S7**
Pier height	7°m	4.23	5.24	1.32	3.35	7.35	2.36	4.35
	11°m	3.25	5.31	2.35	4.19	9.23	3.65	1.26
	13°m	8.36	8.65	4.56	5.42	9.36	9.14	5.92

Table 2: Error percentage for proposed model Δ_{pro} and previous model.

		Error percentage Δ_{pro} and previous model	
		[9]	**[15]**
Pier height	7 m	21.03	40.46
	11 m	23.77	46.93
	13 m	24.68	48.99

displacement. Thus, based on the outcomes, the proposed procedure highlighted and proposed in this paper can convincingly predict an accurate DCTD under real seismic condition.

7 CONCLUSIONS

This paper proposed a new perspective procedure to estimate the $\Delta_{T,DC}$ for RC bridge pier. The influence of new material limit states for RC bridge pier was investigated by integrating new reinforcement strain limit with existing concrete compression strain to predict the DCLS, thus determine the $\Delta_{T,DC}$. This proposed model is integrating a new yield displacement, yield curvature and modified plastic-hinge region into the model. Even though no laboratory experimentation was carried out, an estimate of the accuracy of the proposed model procedure was provided by comparison with the analyses of a 3D FE model subjected to 7 randomly selected ground motions for validation. The results are highlighted below:

1. The newly developed model can be used to predict the damage-control target displacement, $\Delta_{T,DC}$ with reasonable accuracy for the seismic design of the RC bridge piers.
2. The influence of yield stress of transverse reinforcement on bar buckling strain provides a better estimate of DCLSs.
3. The influence of new DCLSs manages to estimate the damage-control target displacement for RC bridge pier with the different LRRs used in the RC bridge pier model.

REFERENCES

[1] Sadan, O.B., Petrini, L. & Calvi, G.M., Direct displacement-based seismic assessment procedure for multi-span reinforced concrete bridges with single-column piers. *Earthquake Engineering & Structural Dynamics*, **42(7)**, pp. 1031–1051, 2013. https://doi.org/10.1002/eqe.2257

[2] Kappos, A.J., Gidaris, I.G. & Gkatzogias, K.I., Problems associated with direct displacement-based design of concrete bridges with single-column piers, and some suggested improvements. *Bulletin of Earthquake Engineering*, **10(4)**, pp. 1237–1266, 2012. https://doi.org/10.1007/s10518-012-9354-y

[3] Reza, S.M., Alam, M.S. & Tesfamariam, S., Seismic performance comparison between direct displacement-based and force-based design of a multi-span continuous reinforced concrete bridge with irregular column heights. *Canadian Journal of Civil Engineering*, **41(5)**, pp. 440–449, 2014. https://doi.org/10.1139/cjce-2012-0278

[4] Calvi, G.M., Priestley, M.J.N. & Kowalsky, M.J., Displacement-based seismic design of bridges. *Structural Engineering International: Journal of the International Association for Bridge and Structural Engineering (IABSE)*, **23(2)**, pp. 112–121, 2013. https://doi.org/10.2749/101686613x13439149157399

[5] Priestley, M.J.N., Calvi, G.M. & Kowalsky, M.J., *Displacement-Based Seismic Design of Structures*, Pavia, Italy: IUSS Press, 2007.

[6] Suarez, V.A., *Implementation of Direct Displacement-Based Design for Highway Bridges*, Ph.D. Thesis, North Carolina State University, 2008.

[7] Mackie, K.R., Wong, J.M. & Stojadinovic, B., Post-earthquake bridge repair cost and repair time estimation methodology. *Earthquake Engineering & Structural Dynamics*, **39**, pp. 281–301, 2010. https://doi.org/10.1002/eqe.942

[8] Mander, J.B., Priestley, M.J.N. & Park, R., Theoretical stress-strain model for confined concrete. *Journal of Structural Engineering*, **114(8)**, pp. 1804–1826, 1988. https://doi.org/10.1061/(asce)0733-9445(1988)114:8(1804)

[9] Kowalsky, M.J., Deformation limit states for circular reinforced concrete bridge columns. *Journal of Structural Engineering*, **126(8)**, pp. 869–878, 2000. https://doi.org/10.1061/(asce)0733-9445(2000)126:8(869)

[10] Goodnight, J.C., Kowalsky, M.J. & Nau, J.M., Strain limit states for circular RC bridge columns. *Earthquake Spectra*, **32(3)**, pp. 1627–1652, 2016. https://doi.org/10.1193/030315eqs036m

[11] Goodnight, J.C., Kowalsky, M.J. & Nau, J.M., Modified plastic-hinge method for circular rc bridge columns. *Journal of Structural Engineering*, **142(11)**, pp. 1–12, 2016. https://doi.org/10.1061/(asce)st.1943-541x.0001570

[12] Karim, M.R.A. & Huang, Z., Estimation of yield displacement for seismic based design of circular RC bridge piers. In *7th Asia Conference on Earthquake Engineering*, 2018.

[13] Suarez, V.A. & Kowalsky, M.J., A stability-based target displacement for direct displacement-based design of bridge piers. *Journal of Earthquake Engineering*, **15(5)**, pp. 754–774, 2011. https://doi.org/10.1080/13632469.2010.534233

[14] Priestley, M.J.N., Seible, F. & Calvi, G.M., *Seismic Design and Retrofit of Bridges*, New York: John Wiley & Sons, 1996.

[15] Kong, C., *Rapid Direct Displacement-Based Assessment Approach for Bridge Structures*, Ph.D. Thesis, North Carolina State University, 2017.

[16] Hernández-Montes, E. & Aschheim, M., An estimate of the yield displacement of coupled walls for seismic design. *International Journal of Concrete Structures and Materials*, **11(2)**, pp. 275–284, 2017. https://doi.org/10.1007/s40069-017-0188-5

[17] Priestley, M.J.N. & Kowalsky, M.J., Direct displacement-based seismic design of concrete buildings. *Bulletin of the New Zealand National Society for Earthquake Engineering*, **33(4)**, pp. 421–444, 2000.

[18] Sheikh, M.N., Tsang, H.H., McCarthy, T.J. & Lam, N.T.K., Yield curvature for seismic design of circular reinforced concrete columns. *Magazine of Concrete Research*, **62(10)**, pp. 741–748, 2010. https://doi.org/10.1680/macr.2010.62.10.741

[19] Dassault Systèmes Simulia Corp, *Abaqus Analysis User's Manual*, Providence, RI, USA, 2016.

[20] Belarbi, A., Zhang, L.X. & Hsu, T.T.C., Constitutive laws of reinforced concrete membrane elements. In *Eleventh World Conference on Earthquake Engineering*, pp. 1–8, 1996.

[21] Cashell, K.A., Elghazouli, A.Y. & Izzuddin, B.A., Experimental and analytical assessment of ductility in lightly reinforced concrete members. *Engineering Structures*, **32(9)**, pp. 2729–2743, 2010. https://doi.org/10.1016/j.engstruct.2010.04.043

[22] CEN, *Eurocode 2: Design of concrete structures (EN1992-1-1)*. Brussels, 2004.

[23] Lubliner, J., Oliver, J., Oller, S. & Oñate, E., A plastic-damage model for concrete. *International Journal of Solids and Structures*, **25(3)**, pp. 299–326, 1989. https://doi.org/10.1016/0020-7683(89)90050-4

[24] Lee, J. & Fenves, G.L., Plastic-damage model for cyclic loading of concrete structures. *Journal of Engineering Mechanics*, **124(8)**, pp. 892–900, 1998. https://doi.org/10.1061/(asce)0733-9399(1998)124:8(892)

[25] Yahya, N.A., *Strategies for Mitigation of the Failure of Concrete Pedestals Supporting Bridge Girder Bearings*, Ph.D. Queensland University of Technology, 2017.

[26] Jankowiak, T. & Lodygowski, T., Identification of parameters of concrete damage plasticity constitutive model. *Foundations of Civil and Environmental Engineering*, **6(1)**, pp. 53–69, 2005.

[27] Lehman, D., Moehle, J., Mahin, S., Calderone, A. & Harry, L., Experimental evaluation of the seismic performance of reinforced concrete bridge columns. *Journal of Structural Engineering*, **130(6)**, pp. 869–879, 2004. https://doi.org/10.1061/(asce)0733-9445(2004)130:6(869)

[28] CEN, *Eurocode 8: Seismic Design of Buildings (EN1998-1)*. Brussels, 2004.